DYNAMIC NUMERICAL SIMULATION
OF THE 6-PGK PARALLEL ROBOT MANIPULATOR

Liviu MOLDOVAN, Adrian GLIGOR, Horatiu-Stefan GRIF, Flaviu MOLDOVAN

"Petru Maior" University of Târgu-Mures, Nicolae Iorga, 1, Târgu-Mures, 540088, Romania
Corresponding author: Liviu MOLDOVAN, E-mail: `liviu.moldovan@ing.upm.ro`

Abstract. In this paper we discuss the 6-PGK innovative structure of a spatial parallel robot with 6 degrees of freedom. We devised a complete model for the dynamic behavior of the robot which is defined analytically. It allows the evaluation of the robot and aids the design process. The robot is evaluated via the analysis of actuator force index which allows all the actuators of the manipulator to be compared on the same dimensionless scale and to select it properly in the design process. Three sets of tests are performed on the most common trajectories used in industrial applications, consisting in linear and circular motions. The results of the numerical tests that are presented provide some insight to the dynamic behavior of the parallel robot manipulator.

Key words: parallel robot manipulator, degree of freedom, dynamic model, actuator force index.

1. INTRODUCTION

Parallel robot manipulators are closed-loop mechanisms which control the position and the orientation of the end-effector via a mechanical system constituted by a number of links arranged in parallel. The synchronized motion of these links produces the desired motion of the end-effector. For the past several decades, parallel robot manipulators have been found for extensive applications including assembly work, flexible manufacturing, machine tools, piezoelectric transducers, sensors, haptic devices, bionic eye mechanisms, spray painting, etc. [1, 2].

Performance is a critical topic for the further improvement of parallel robot manipulators. Improving the overall performance of parallel robot manipulators is the bridge to connect the academia and industry for the great development and real-world application.

In order to evaluate the performance of a parallel robot, various indexes are used: the polytrope force, the out-of-plane stability, the performance visualization, the finite element analysis, the genetic algorithms and the artificial neural networks as an intelligent optimization tool for the dimensional synthesis of the spatial six degree-of-freedom, the performance atlases, the performance index defined as the maximum acceptable distance between the mobile platform geometric center and the center of mass of the set consisting of the platform and a payload, etc. [3, 4]. For the efficient computation of the solution set diverse software packages which implement various algorithms are used. Such an example is represented by the algorithm based on homotopy continuation [5].

The purpose of this paper is to study the performance of the 6-PGK parallel robot manipulator using the actuator force index as index of robot performance, on various set of parameters and to provide some insight to the dynamic behavior that is useful in the design process. The objective is to use the conservative estimates of parameters in order to obtain the worst case actuator requirements.

2. THE 6-PGK PARALLEL ROBOT MANIPULATOR

2.1. The geometric structure

The basic geometric structure of the 6-PGK parallel robot manipulator developed at "Petru Maior" University consists in a mobile platform (supporting the end-effector) connected to the adjacent links at six distinct points C_i ($i = 1,2,\dots,6$) located at the distances l_i from the *oz* axis and symmetrical positioned at the level III, by cardan

kinematic pairs, which form the δ_i angles with the ox axis (Fig. 1) [6, 7]. The orientations of the two Cardan joints' rotational axes are located in the plane of the mobile platform and perpendicular to thereto.
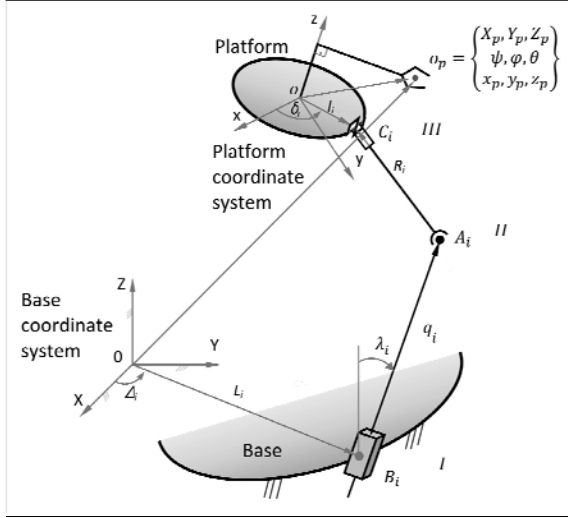

Fig. 1 – The structure of the 6-PGK parallel robot [6].

Each leg has an actuated translational kinematic pair at level I located at the distances L_i from the OZ axis, that are symmetrically positioned by the angles Δ_i with the OX axis and a spherical kinematic pair at level II. The translational kinematic pairs form the angles λ_i with the vertical axis in points B_i, varying in the interval of $[0°–90°]$. The location (position and orientation) of the end-effector and of the manipulated object are expressed in the base coordinate system $OXYZ$ by the generalized coordinates of the manipulated object X_p, Y_p, Z_p, ψ, φ, θ denoted q_{p_j} ($j = 1,2,…,6$), and in the platform coordinate system $oxyz$ by the x_p, y_p, z_p coordinates. The constructive dimensions of the parallel mechanism are $L_i = 0.4$ m, $l_i = 0.27$ m, $R_i = 0.26$ m, $\delta_I = (i-1)60°$, $\Delta_I = (i–1)60°$, $x_p = 0$, $y_p = 0$, $z_p = 0.25$ mm ($I = 1,…,6$).

The displacements in the actuated translational kinematic pairs (actuators displacements) are the generalized coordinates of the parallel robot q_i ($I = 1,…,6$). The range of motion is restricted by the workspace limits of the mechanism, which seems to be like a turned teapot with six feet [8].

2.2. Inverse kinematics

Motion control of the robot needs an inverse kinematics which is described as a transformation of the position and orientation of the end-effector into the control variables driven by actuators. The vector equations, expressed for each leg of the robot (Fig. 1) [6] are:

$$\overline{A_i C_i} = \overline{Oo}_p - \overline{OB}_i + o\overline{C}_i - \overline{oo}_p - \overline{B_i A_i} \quad (i = 1, 2, ..., 6) \tag{1}$$

which in matrix form are:

$$^O\big[A_i C_i\big] = {}^O\big[Oo_p\big] - {}^O\big[OB_i\big] + [R]\,{}^o\big[oC_i\big] - [R]\,{}^o\big[oo_p\big] - {}^O\big[B_i A_i\big] \quad (i = 1, 2, ..., 6) \tag{2}$$

where O denotes the fixed frame $OXYZ$ and o denotes the mobile frame $oxyz$ assigned to the mobile platform. $[R]$ is the rotational matrix that relates the coordinates fixed in mobile frame to the base coordinates $OXYZ$:

$$[R] = \begin{bmatrix} \alpha' & \alpha'' & \alpha''' \\ \beta' & \beta'' & \beta''' \\ \gamma' & \gamma'' & \gamma''' \end{bmatrix} = \begin{bmatrix} C\psi C\varphi - S\psi C\theta S\varphi & -C\psi S\varphi - S\psi C\theta C\varphi & S\psi S\theta \\ S\psi C\varphi + C\psi C\theta S\varphi & -S\psi S\varphi + C\psi C\theta C\varphi & -C\psi S\theta \\ S\theta S\varphi & S\theta C\varphi & C\theta \end{bmatrix} \tag{3}$$

By squaring equation (2), where:

$$^O\big[Oo_p\big] = \big[X_p, Y_p, Z_p\big]^T ; \; {}^o\big[oo_p\big] = \big[x_p, y_p, z_p\big]^T ; \; {}^o\big[oC_i\big] = \big[l_i C\delta_i, l_i S\delta_i, 0\big]^T \quad (i = 1, 2, ..., 6);$$

$$^O\big[OB_i\big] = \big[L_i C\Delta_i, L_i S\Delta_i, 0\big]^T \; (i = 1, 2, ..., 6); {}^O\big[B_i A_i\big] = \big[q_i S\lambda_i S\Delta_i, -q_i S\lambda_i C\Delta_i, q_i C\lambda_i\big]^T \quad (i = 1, 2, ..., 6) \tag{4}$$

and T denotes the transpose matrix, it results:

$$q_i^2 - 2q_i\Big\{\Big[X_p - L_i C\Delta_i - \big(x_p - l_i C\delta_i\big)\alpha' - \big(y_p - l_i S\delta_i\big)\alpha'' - z_p\alpha'''\Big]S\lambda_i S\Delta_i - \Big[Y_p - L_i S\Delta_i - \big(x_p - l_i C\delta_i\big)\beta' - \big(y_p - l_i S\delta_i\big)\beta'' -$$

$$- z_p\beta'''\Big]S\lambda_i C\Delta_i + \Big[Z_p - \big(x_p - l_i C\delta_i\big)\gamma' - \big(y_p - l_i S\delta_i\big)\gamma'' - z_p\gamma'''\Big]C\lambda_i\Big\} + \Big[X_p - L_i C\Delta_i - \big(x_p - l_i C\delta_i\big)\alpha' - \big(y_p - l_i S\delta_i\big)\alpha'' - \tag{5}$$

$$- z_p\alpha''\Big]^2 + \Big[Y_p - L_i S\Delta_i - \big(x_p - l_i C\delta_i\big)\beta' - \big(y_p - l_i S\delta_i\big)\beta'' - z_p\beta'''\Big]^2 + \Big[Z_p - \big(x_p - l_i C\delta_i\big)\gamma' - \big(y_p - l_i S\delta_i\big)\gamma'' - z_p\gamma'''\Big]^2 - R_i^2 = 0$$

$(i = 1,2, \ldots ,6)$ the in-out equations of the robot that are obtained, in the form:

$$q_i^2 - 2b_i q_i + c_i = 0 \quad (i = 1, 2, ..., 6). \tag{6}$$

that is a system of six second order equations in q_i, with the solution $(q_i)_{1,2}$ $(i = 1,2,...,6)$. It means that for the same location of the mobile platform two configurations of the robot's legs are possible. The existence of the solutions must be verified because in practice, it is sometimes possible to obtain only a sole solution:

$$q_i^m \le \left(q_i\right)_{1,2} \le q_i^M \quad (i = 1,2,...,6), \tag{7}$$

where q_i^m and q_i^M are the minimum and the maximum values of the robot generalized coordinates.

2.3. Inverse instantaneous kinematics

The inverse instantaneous kinematic problem aims to compute the generalized velocities of the parallel robot $\dot{q}_i$ $(i = 1,2,...,6)$ given the manipulated object velocities $\dot{X}_p, \dot{Y}_p, \dot{Z}_p, \dot{\psi}, \dot{\varphi}, \dot{\theta}$ denoted $\dot{q}_{p_i}$ $(j = 1,2,... ,6)$, as follows [6]:

$$\dot{q}_i = \sum_{j=1}^{6} l_{ij} \dot{q}_{p_j} = l_{i1}\dot{X}_p + l_{i2}\dot{Y}_p + l_{i3}\dot{Z}_p + l_{i4}\dot{\psi} + l_{i5}\dot{\varphi} + l_{i6}\dot{\theta} \quad (i = 1,2,...,6). \tag{8}$$

By deriving the equations (6), the robot generalized velocities are deduced:

$$\dot{q}_i = \left(2\dot{b}_i q_i - \dot{c}_i\right)\big/2\left(q_i - b_i\right) \quad (i = 1,2,...,6). \tag{9}$$

By comparing the equations (8) and (9) the l_{ij} $(i = 1,2,...,6; j = 1,2,...,6)$ terms of the inverse Jacobian matrix are obtained.

The angular velocity terms in *OXYZ* system are:

$$\omega_X = \dot{\varphi}S\theta S\psi + \dot{\theta}C\psi, \quad \omega_Y = -\dot{\varphi}S\theta C\psi + \dot{\theta}S\psi, \quad \omega_Z = \dot{\psi} + \dot{\varphi}C\theta. \tag{10}$$

By differentiating equation (10), the angular acceleration projections of the manipulated object are obtained:

$$\varepsilon_x = \ddot{\varphi}S\theta S\psi + \ddot{\theta}C\psi + \dot{\varphi}\dot{\theta}C\theta S\psi + \dot{\varphi}\dot{\psi}S\theta C\psi - \dot{\theta}\dot{\psi}S\psi, \quad \varepsilon_y = -\ddot{\varphi}S\theta C\psi + \ddot{\theta}S\psi - \dot{\varphi}\dot{\theta}C\theta C\psi + \dot{\varphi}\dot{\psi}S\theta S\psi + \dot{\theta}\dot{\psi}S\psi,$$
$$\varepsilon_z = \ddot{\psi} + \ddot{\varphi}C\theta - \dot{\varphi}\dot{\theta}S\theta. \tag{11}$$

2.4. Equations of motion

The Lagrangian formulation describes the behavior of the parallel robot in terms of machine work and energy stored in the system rather than in terms of forces and moments of the individual legs involved [9, 10]. The Lagrangian equations of motion of the 6-degree-of-freedom parallel robot are:

$$\frac{\mathrm{d}}{\mathrm{d}t}\left(\frac{\partial E_c}{\partial \dot{q}_{p_j}}\right) - \frac{\partial E_c}{\partial q_{p_j}} = Q_j \quad (j = 1,2,...,6) \tag{12}$$

where E_c, q_{p_j} and Q_j are the kinetic energy, the generalized coordinates of the manipulated object and the generalized forces, respectively.

Since no closed-form solution exists for the forward kinematic problem of the parallel robot, Cartesian position and orientation of the mobile object cannot be expressed in terms of the parallel robot generalized coordinates. Consequently, the generalized coordinates from equations (12) are selected to be the manipulated object generalized coordinates. The kinetic energy of the elements A_iC_i $(i = 1,2,...,6)$ can be neglected due to the small masses in comparison with the other elements of the parallel robot (Fig. 1). The total kinetic energy of the parallel robot consists of the kinetic energy created from the general motion of the mobile plat-

form, of the gripper and of the manipulated object and of the kinetic energy produced by the motor links translational motion along the prismatic joints:

$$E_c = \frac{1}{2}\sum_{k=1}^{3}\sum_{l=1}^{3} J_{kl}\omega_k\omega_l + \frac{1}{2}\sum_{k=1}^{3}(m_o + m_p)\dot{q}_{p_k}^2 + \frac{1}{2}\sum_{i=1}^{6} m_i\dot{q}_i^2, \tag{13}$$

where m_0 represents mobile platform mass, m_p represents gripper and manipulated object mass, m_i are the motor links masses and J_{kl} are the inertia matrix elements $^O[J*]$ in terms of the coordinate system $OXYZ$:

$$^O[J*] = [R]\,^o[J*][R]^T, \tag{14}$$

where $^O[J*]$ represents inertia matrix in the coordinate system $oxyz$, whose axes are main axes of the mobile platform. The manipulated object and the gripper are considered to be a point of mass m_p and coordinates x_p, y_p, z_p in the system $oxyz$.

By identification, from the virtual work of the robot mechanism it results:

$$\delta L = \sum_{i=1}^{6}\left(Q_{m_i}\delta q_i - m_i g \delta Z_{G_i}\right) - m_p g \delta Z_p - m_o g \delta Z_o = Q_1\delta X_p + Q_2\delta Y_p + Q_3\delta Z_p + Q_4\delta\psi + Q_5\delta\varphi + Q_6\delta\theta, \tag{15}$$

where $Z_{G_i} = (q_i - l_i)C\lambda_i$, $(i = 1,2,...,6)$ are the motor elements mass centers coordinates, the generalized forces that act on the robot mechanism are obtained:

$$Q_1 = \sum_{i=1}^{6}\left(Q_{m_i} - m_i gC\lambda_i\right)l_{i1}; \quad Q_2 = \sum_{i=1}^{6}\left(Q_{m_i} - m_i gC\lambda_i\right)l_{i2}, \quad Q_3 = \sum_{i=1}^{6}\left(Q_{m_i} - m_i gC\lambda_i\right)l_{i3} - Mg \; ; Q_4 = \sum_{i=1}^{6}\left(Q_{m_i} - m_i gC\lambda_i\right)l_{i4},$$

$$Q_5 = \sum_{i=1}^{6}\left(Q_{m_i} - m_i gC\lambda_i\right)l_{i5} + m_o g\left(x_p S\theta C\varphi - y_p S\theta S\varphi\right), \quad Q_6 = \sum_{i=1}^{6}\left(Q_{m_i} - m_i gC\lambda_i\right)l_{i6} + m_o g\left(x_p C\theta S\varphi + y_p C\theta C\varphi - z_p S\theta\right) \tag{16}$$

where Q_{m_i} are the robot motor generalized forces, g is the gravity acceleration and $M = m_0 + m_p$.

By using equations (12) and (13), after some mathematical computations the following parallel robot motion equations are obtained:

$$\frac{1}{2}\sum_{k=1}^{3}\sum_{l=1}^{3}\dot{J}_{kl}\left(\frac{\partial\omega_k}{\partial\dot{q}_{p_j}}\omega_l + \omega_k\frac{\partial\omega_l}{\partial\dot{q}_{p_j}}\right) - \frac{1}{2}\sum_{k=1}^{3}\sum_{l=1}^{3}\frac{\partial J_{kl}}{\partial q_{p_j}}\omega_k\omega_l + \frac{1}{2}\sum_{k=1}^{3}\sum_{l=1}^{3} J_{kl}\left[\frac{\mathrm{d}}{\mathrm{d}t}\left(\frac{\partial\omega_k}{\partial\dot{q}_{p_j}}\right)\omega_l + \frac{\partial\omega_k}{\partial\dot{q}_{p_j}}\varepsilon_l + \varepsilon_k\frac{\partial\omega_l}{\partial\dot{q}_{p_j}} + \right.$$

$$\left. + \omega_k\frac{\mathrm{d}}{\mathrm{d}t}\left(\frac{\partial\omega_l}{\partial\dot{q}_{p_j}}\right)\omega_l\right] + M\sum_{k=1}^{3}\ddot{q}_{p_k}\frac{\partial\dot{q}_{p_k}}{\partial\dot{q}_{p_j}} + \sum_{i=1}^{6} m_i\left[\ddot{q}_i\frac{\partial\dot{q}_i}{\partial\dot{q}_{p_j}} + \dot{q}_i\frac{\mathrm{d}}{\mathrm{d}t}\left(\frac{\partial\dot{q}_i}{\partial\dot{q}_{p_j}}\right)\right] - \frac{1}{2}\sum_{k=1}^{3}\sum_{l=1}^{3} J_{kl}\left(\frac{\partial\omega_k}{\partial q_{p_j}}\omega_l + \omega_k\frac{\partial\omega_l}{\partial q_{p_j}}\right) - \tag{17}$$

$$- \sum_{i=1}^{6} m_i\dot{q}_i\frac{\partial\dot{q}_i}{\partial q_{p_j}} = Q_j, \quad (j=1,2,...,6).$$

The motion dynamic equations (17) obtained by Lagrange method are composed of three terms: inertial, centrifugal and Coriolis, and gravitational [11].

The relationship between [Q]-generalized forces vector, [Q_m]-generalized motor forces vector, by means of [J]-inverse Jacobian matrix is:

$$[Q_m] = [J][Q]. \tag{18}$$

3. MOTION AND TASK PLANNING FOR TESTING

Two different types of motions or tasks are used for robot dynamic testing in Matlab simulation software. The platform is used in a machining process to support and move workpieces. A full groove is cut with a four tooth end mill. The workpiece is to be taken through rectilinear and curvilinear motion as explained below.

The first motion to be used for machining the workpiece is a rectilinear motion parallel to the *XY* plane at a distance Z_p from the base, as shown in Fig. 2a, along the axis of translation *w* which is at an angle α with the *X* axis, as shown in Fig. 2b. The platform starts moving from point C_{start}, performs a ΔS displacement along the direction of motion in a period of time *T* and completes its motion at point C_{stop}. The workpiece is machined through the complete motion.
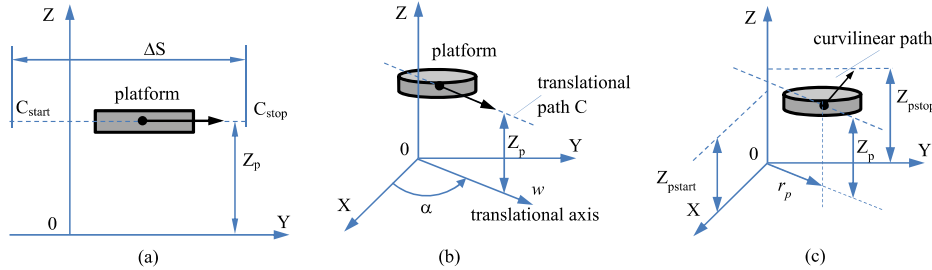
Fig. 2 a – Rectilinear motion for machining; b. Axis of translation for the platform; c. Curvilinear motion for machining.

The second motion to be used for machining the workpiece is a curvilinear motion. The trajectory has a curvature radius r_p, the axis of rotation *OZ*, starting at the height Z_{pstart} and ending at Z_{pstop}, as shown in Fig. 2c. The initial orientation of the platform is 0°, and it rotates 180° in a period of time *T* to end. The workpiece is machined through the complete motion and the cutting forces are tangent to the path at all times.

4. TEST CASES RESULTS AND DISCUSSION

The effect of geometric variations is explored by changing the height Z_p and the angles λ_i, then variations of the motion planning parameters is examined by reducing the time period *T* required for completing the motion.

The required actuator forces are calculated for each test by the simulation program and displayed. One important condition is that the actuator forces requirements must not exceed the maximum force capacity. When this happens, the system is operating in a condition known as actuator singularity and the desired motion cannot be produced by the manipulator. The possibility of actuator singularity appearance is monitored with the actuator force index parameter:

$$AFI = \left[\left(Q_{\max} - Q_m \right) / Q_{\max} \right] \times 100, \tag{19}$$

where: Q_{max} represents the actuator maximum force capacity and Q_m is the required actuator force.

The above equation is similar to the definition of some performance indices used in the area of control theory. The use of the actuator force index *AFI* allows all the actuators of the manipulator to be compared on the same dimensionless scale which might be somewhat difficult by just using the actuator force plots. The force index simplifies identifying actuator saturation; the smaller the force index, the closer the actuator is being saturated. This index also allows the designer to avoid overdesigning or understanding when selecting the actuators.

4.1. Test cases with geometric variations

The first test cases involve a rectilinear motion of the platform as discussed in Fig. 2a, b. In the group of tests the height of the platform Z_p was increased from $Z_{p1} = 0.3$ m, $Z_{p2} = 0.5$ m up to $Z_{p3} = 0.7$ m.

For the rectilinear motion it can be seen that as the height is increased there is an increase in module of the force requirements for all the actuators (Fig. 3a). This is seen more clearly in the actuators force index plots when *AFI* is nearest to 0, which happens for the extreme values of the actuator forces (Fig. 3b).

This suggests that the general force requirements increase with the height. The lower the height, the greater horizontal force components which are desirable for balancing the effect of an external load, such as the cutting force.
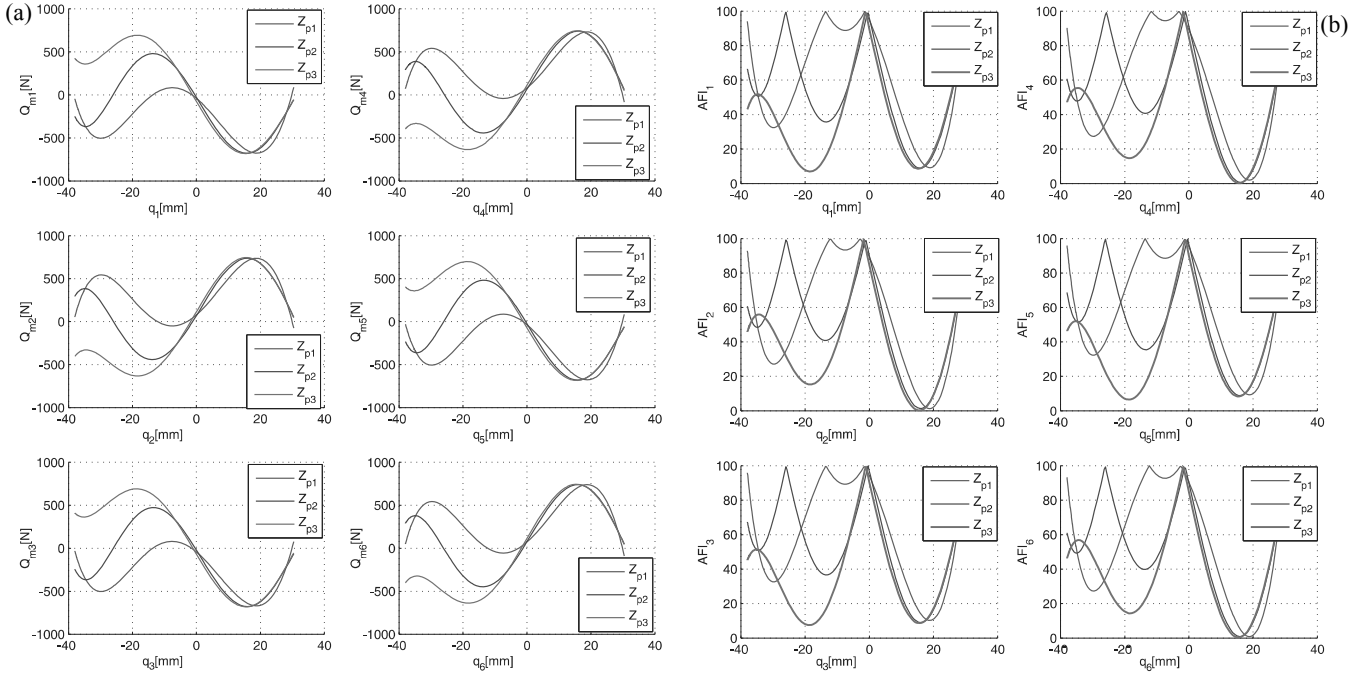
Fig. 3 – Effects of the platform height on the: a) actuator forces; b) actuator force index, rectilinear motion.

The second test case uses the curvilinear motion described in Fig. 2c, and the reference height of the platform is increased between 0.3 m, 0.5 m up to 0.7 m, the angle λ is zero and the time period T is 20 seconds. The results of these tests are shown in Fig. 4a, 4b.
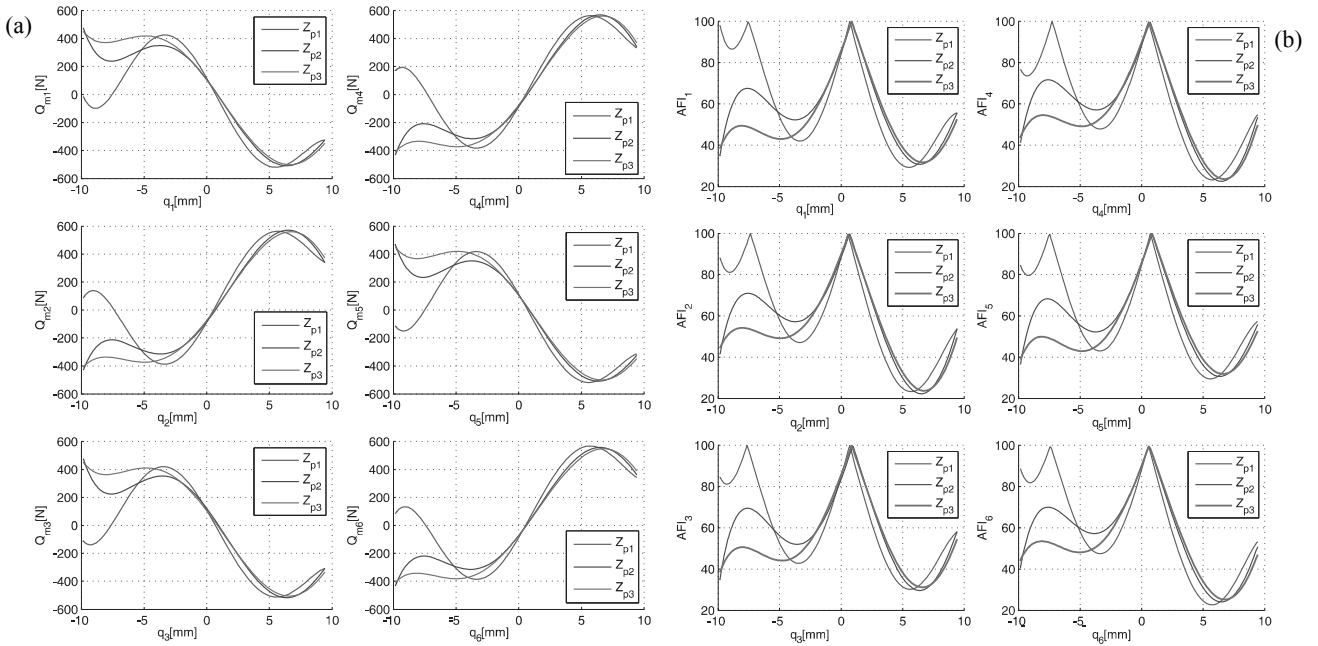

Fig. 4 – Effects of the platform height on the: a) actuator forces; b) actuator force index, curvilinear motion.

The effects of changing the height for the curvilinear motion are similar with the results obtained for the rectilinear motion. For the curvilinear motion as the height is increased, the overall force requirements are higher.

The next set of tests consists of changing the angle $\lambda_1 = 0°$, $\lambda_2 = 30°$, $\lambda_3 = 60°$ while keeping the platform at a fixed height of $Z_p = 0.3$ m and the time period T equal to 20 seconds. The results of the rectilinear and curvilinear motions are shown in Figs. 5.a,b and 6.a,b respectively.
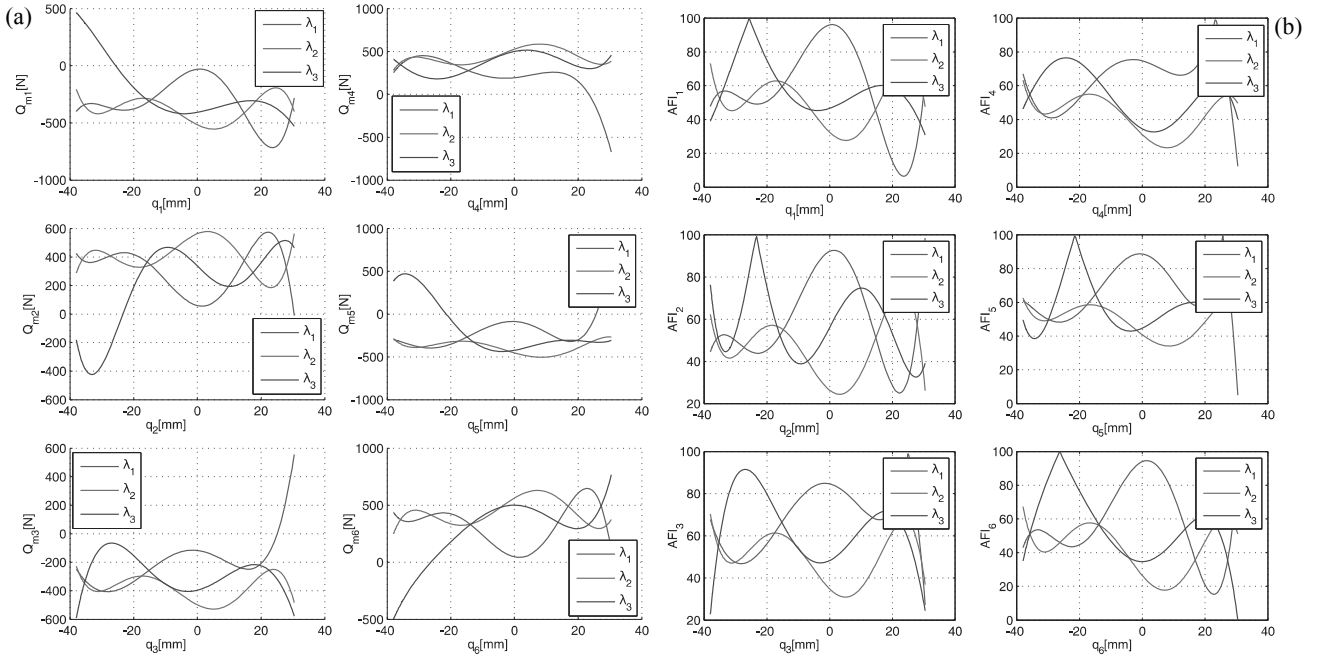
Fig. 5 – Effects of the angle λ on the: a) actuator forces; b) actuator force index, rectilinear motion.
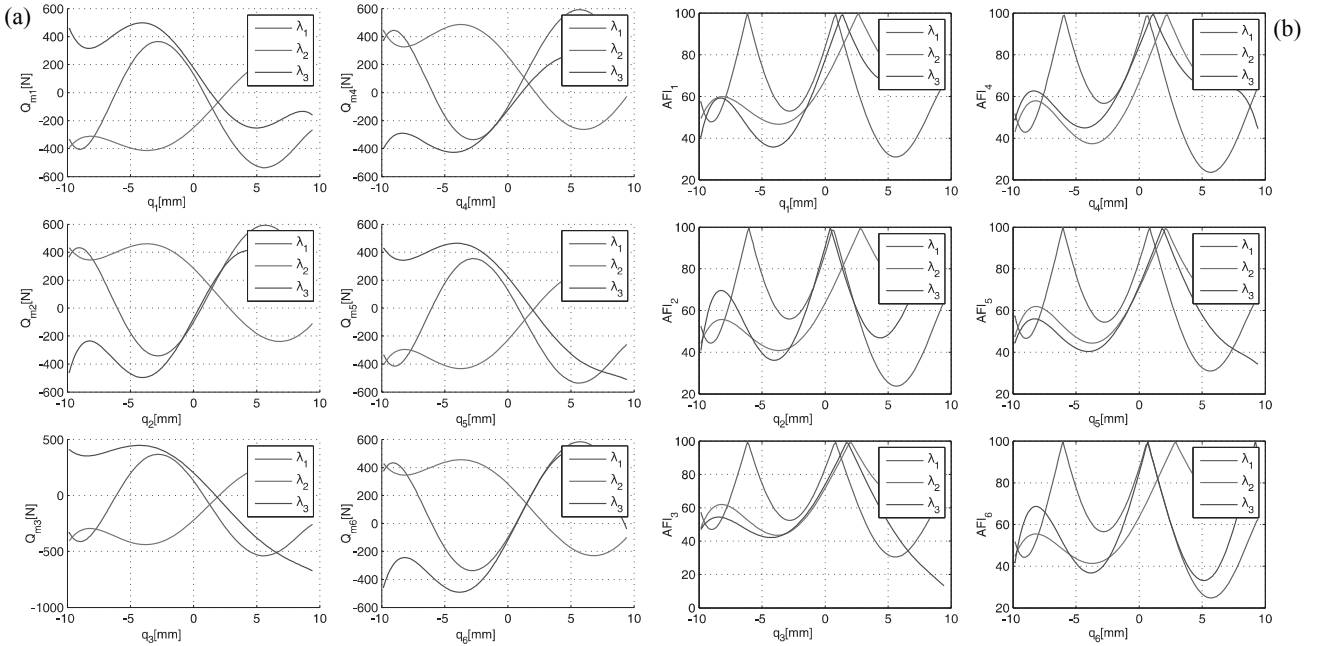

Fig. 6 – Effects of the angle λ on the: a) actuator forces; b) actuator force index, curvilinear motion.

These plots indicate that increasing the angle λ between the actuators and the normal to the base platform, requires an increasing of general actuator force. The increase of λ angle increases the force components for the actuators in the higher plane.

4.2. Test cases with variations of motion planning parameters

The effects of motion planning parameters variations are examined by reducing the time period T required for completing the motion. This set of tests is conducted considering the variations of the T time period. A shorter time period leads to a faster platform movement.

The results of the tests for the rectilinear and curvilinear motions are shown in Figs. 7.a,b and 8.a,b respectively. It can be seen that the reduction of the time period from 20 seconds, 10 seconds and 1 second does not produce any noticeable changes in the force requirements.
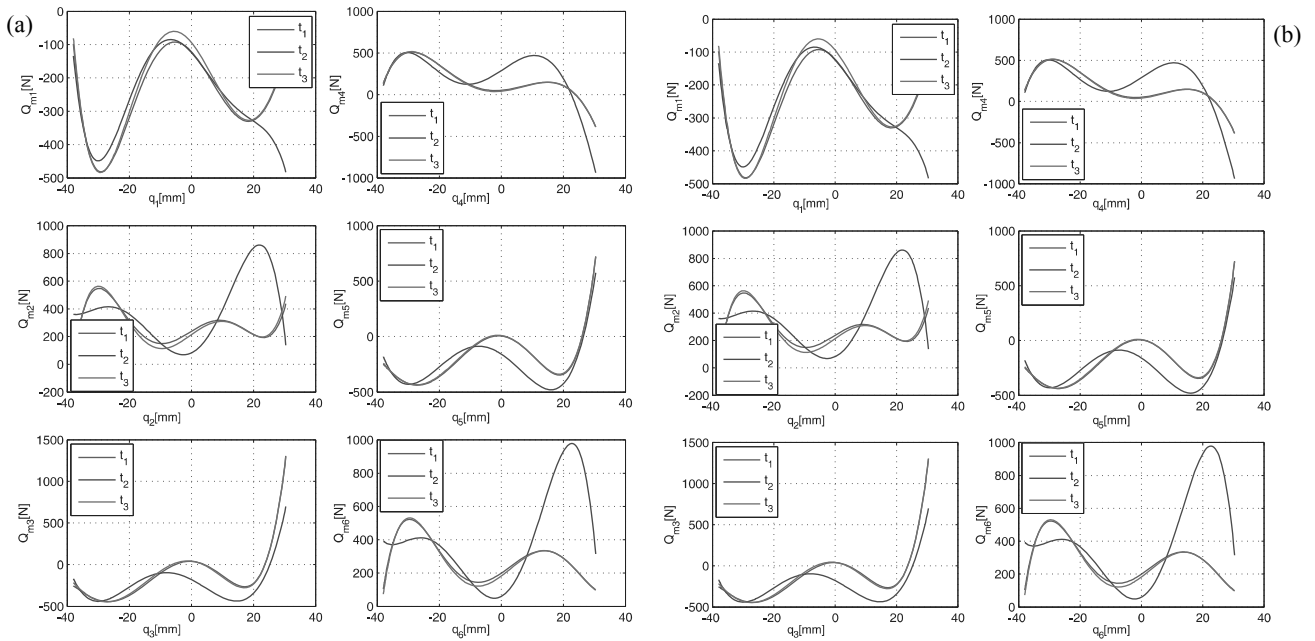

Fig. 7 – Effects of the time period on the: a) actuator forces; b) actuator force index, rectilinear motion.
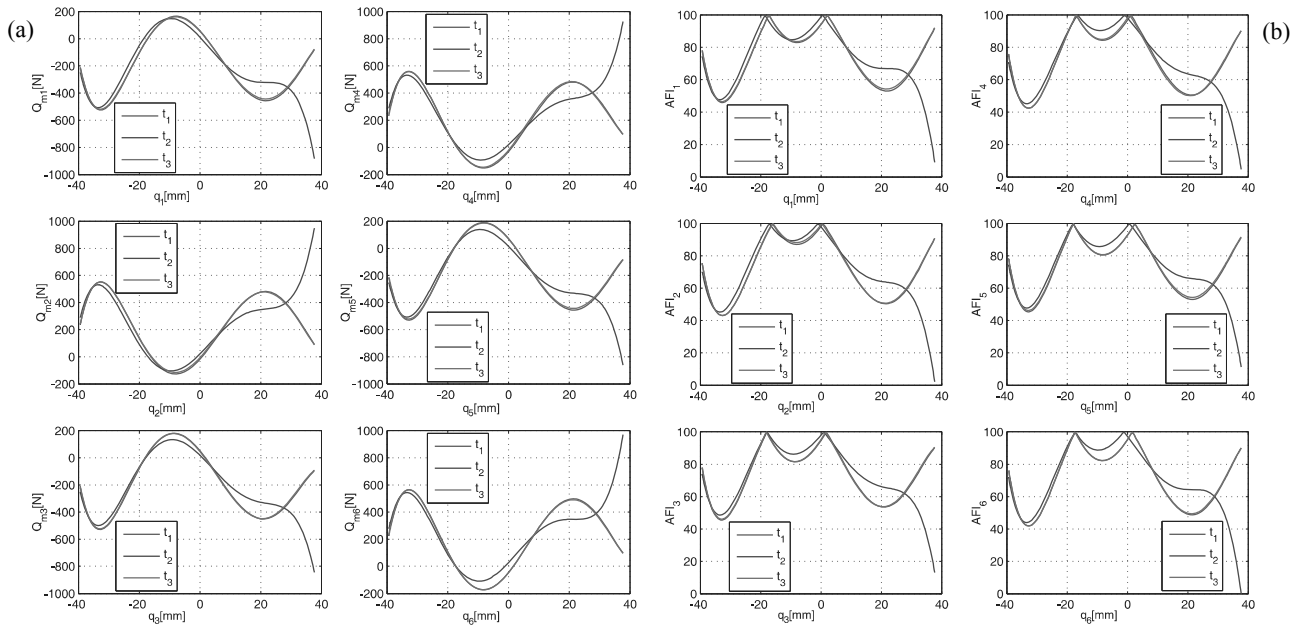

Fig. 8 – Effects of the time period on the: a) actuator forces; b) actuator force index, curvilinear motion.

The platform moves faster as the time period is shorter, and the velocity and acceleration of the connectors will increase. This will increase the magnitude of the tangential, Cori-olis and centrifugal coupling wrenches of the actuators, since they are functions of the kinematic state of the system, among other things.

Since these wrenches are a function of the kinematic state, one would expect a noticeable increase in the actuator force requirements as the platform moves faster. In the test results this trend is not observed. One possible explanation is that the magnitudes of the angular velocities and acceleration vectors are small for the motions tested.

5. CONCLUSIONS

In this paper we present the new 6-PGK spatial parallel robot with 6 degrees of freedom. In order to evaluate the robot and fulfill the design process a complete dynamic model based on the Lagrange method was defined. The numerical evaluation phase is carried out by exploiting the concept of actuator force index which is essentially a dimensionless performance index that allows the designer to avoid overdesigning or to appropriate actuators selection. This index indicates when an individual actuator saturates but does not indicate for how long it stays saturated and does not take into account the rest of the actuators. The designer has to compare all the force index plots for one design with all the force index plots of a competing design in order to select the most suitable design.

Tests are done on two different trajectories which are most common in industrial applications.

In a first set of tests it is demonstrated for both trajectories that the general force requirements increase with the height Z_p on which the task is performed. The lower the height, the batter the capacity of the parallel robot manipulator to balance the effect of external load.

The next set of tests consists in changing the angle λ between the actuators and the normal to the base platform. The results indicate that increasing λ angle increases the general actuator force requirements. The increase of angle λ increases the force components for the actuators in the higher plane.

The third set of tests was conducted using variations of the time period T for the same task. It is demonstrated that the reduction of the time period does not produce any noticeable changes in the force requirements.

The equations of motion depend on a large set of parameters that can vary. This underlines the high importance of extensive testing with different sets of geometric parameters, system parameters, motions and tasks in order to carefully study the effects of coupling. These results provide some insight on the dynamic behavior of a developed system and how it is affected by different factors.

REFERENCES

1. AGELI, M., NESTINGER, S.S., Comprehensive closed-form solution for the reachable workspace of 2-RR planar parallel mechanisms, Mech Mach. Theory, **74**, pp. 102-116, 2014.
2. LIU, X.J., LI, J., ZHOU, Y,H., Kinematic optimal design of a 2-degree-of-freedom 3-parallelogram planar parallel manipulator, Mechanism and Machine Theory, **87**, pp. 1-17, 2015.
3. SERIANI, S., GALLINA, P., A Storable Tubular Extendible Member (STEM) parallel robot: Modelization and evaluation, Mechanism and Machine Theory, **90**, pp. 95-175, 2015.
4. ZHANG, D., GAO, Z., Performance analysis and optimization of a five-degrees-of-freedom compliant hybrid parallel micromanipulator, Robotics and Computer-Integrated Manufacturing, **34**, pp. 20-29, 2015.
5. ABBASNEJAD, G.; CARRICATO, M., Direct Geometrico-static Problem of Underconstrained Cable-Driven Parallel Robots with n Cables., IEEE Transactions on Robotics, 31(2), pp. 468-478, 2015.
6. MOLDOVAN, L., *Trajectory Errors of the 6-PGK Parallel Robot*, IEEE Proc. of First Intl. Conf. CANS '08, pp. 31-37, 2008.
7. MOLDOVAN, L., Parallel mechanism with six degrees of freedom for robot construction, Patent Invention, OSIM No. 128018, 2016.
8. MOLDOVAN, L., *Geometrical Method for Description of the 6-PGK Parallel Robot's Workspace*, IEEE Proc. of First Intl. Conf. CANS '08, pp. 45-51, 2008.
9. STAICU, S., *Inverse dynamics of the spatial 3-RPS parallel robot*, Proceedings of the Romanian Academy Series A – Mathematics Physics Technical Sciences Information Science, **13**, *1*, pp. 62-70, 2012.
10. PLITEA, N., SZILAGHYI, A., COCOREAN, D., COVACIU, F., VAIDA, C., PISLA D., *Inverse dynamic modeling of a parallel robotic system for brachytherapy*, Proceedings of the Romanian Academy Series A – Mathematics Physics Technical Sciences Information Science, **17**, *1*, pp. 67-75, 2016.
11. MOLDOVAN, L., GRIF, H.-S., GLIGOR, A., *ANN Based Inverse Dynamic Model of the 6-PGK Parallel Robot Manipulator*, Int. J. Comput. Commun., **11**, *1*, pp. 90-104, 2016.